LETTERS

The protein kinase A anchoring protein mAKAP coordinates two integrated cAMP effector pathways

Kimberly L. Dodge-Kafka[1]†, Joseph Soughayer[1], Genevieve C. Pare[2], Jennifer J. Carlisle Michel[1], Lorene K. Langeberg[1], Michael S. Kapiloff[2] & John D. Scott[1]

Cyclic adenosine 3′, 5′-monophosphate (cAMP) is a ubiquitous mediator of intracellular signalling events. It acts principally through stimulation of cAMP-dependent protein kinases (PKAs)[1,2] but also activates certain ion channels and guanine nucleotide exchange factors (Epacs)[3]. Metabolism of cAMP is catalysed by phosphodiesterases (PDEs)[4,5]. Here we identify a cAMP-responsive signalling complex maintained by the muscle-specific A-kinase anchoring protein (mAKAP) that includes PKA, PDE4D3 and Epac1. These intermolecular interactions facilitate the dissemination of distinct cAMP signals through each effector protein. Anchored PKA stimulates PDE4D3 to reduce local cAMP concentrations, whereas an mAKAP-associated ERK5 kinase module suppresses PDE4D3. PDE4D3 also functions as an adaptor protein that recruits Epac1, an exchange factor for the small GTPase Rap1, to enable cAMP-dependent attenuation of ERK5. Pharmacological and molecular manipulations of the mAKAP complex show that anchored ERK5 can induce cardiomyocyte hypertrophy. Thus, two coupled cAMP-dependent feedback loops are coordinated within the context of the mAKAP complex, suggesting that local control of cAMP signalling by AKAP proteins is more intricate than previously appreciated.

Spatiotemporal control of cAMP flux requires the concerted action of adenylyl cyclases that synthesize cAMP, and phosphodiesterases that locally metabolize it into 5′-AMP (ref. 4). PDE binding proteins target distinct isozymes to specific subcellular sites[5–7]. In cardiomyocytes, mAKAP assembles a negative feedback loop containing PDE4D3 and PKA at the perinuclear membrane[8]. PKA phosphorylation of Ser 13 on PDE4D3 increases binding to mAKAP[9], whereas phosphorylation (of PDE4D3 by PKA) of Ser 54 enhances cAMP catabolism[10]. This configuration may generate local fluctuations in cAMP and pulses of compartmentalized PKA activity[11].

Here we used fluorescent reporters of PKA activity to test this model in cultured human and rat cells[12]. AKAR2, a reversible A-kinase activity reporter[31], is an improved version of AKAR1. This chimaeric protein consists of cyan fluorescent protein (CFP), a consensus PKA substrate sequence, a forkhead-associated (FHA) domain that binds phosphoamino acids, and the yellow fluorescent protein (YFP) citrine (Fig. 1a). PKA phosphorylation of the consensus site engages the FHA domain, permitting fluorescence resonance energy transfer (FRET) between the fluorescent moieties. Two modified AKAR2 reporters were generated: AKAR–PKA, which recruits PKA by means of a consensus anchoring sequence (Fig. 1b), and AKAR–PKA–PDE, which recruits PKA and tethers PDE4D3 through a binding site derived from mAKAP (Fig. 1c). HeLa cells expressing AKAP–PKA showed a rapid and sustained elevation of FRET on cAMP stimulation (Fig. 1b; red trace in Fig. 1d (n = 10); Supplementary Video 1). In contrast, cells expressing

AKAR–PKA–PDE showed a transient and less robust FRET response (Fig. 1c; green trace in Fig. 1d (n = 13); Supplementary Video 2). The PKA antagonist H89 blocked all cAMP-dependent FRET changes (Fig. 1d). PKA activity was unaffected by the PDE3 inhibitor milrinone (10 μM). However, suppression of PKA activity was prevented when the same cells received the PDE4 inhibitor rolipram (1 μM) (Fig. 1e, n = 10; Supplementary Video 3). Thus, recruitment of a PDE4 terminates activation of anchored PKA in the context of the AKAR–PKA–PDE reporter.

ERK kinases phosphorylate PDE4D3 on Ser 579 to suppress phosphodiesterase activity[13]. We predicted that mAKAP might incorporate an ERK kinase module to counterbalance the anchored PDE4D3. Accordingly, sustained elevation of FRET on cAMP stimulation was observed in HeLa cells expressing AKAR–PKA–PDE plus constitutively active MEK, a kinase upstream of ERKs (black trace in Fig. 1f, n = 11). From this, we suggest that ERK activity suppresses anchored phosphodiesterase activity. Complementary studies were performed in cultured rat neonatal ventriculocytes (RNVs). Treatment with 10% fetal calf serum activated ERK before immunoprecipitation of the mAKAP complex. The associated PDE activity was attenuated by 52 ± 9% (n = 4, P < 0.0002) compared to unstimulated controls (Fig. 1g, column 2). The MEK inhibitor PD98059 (20 μM) blocked this effect (Fig. 1g, column 3, P < 0.002). Equivalent amounts of PDE4D3 were co-purified with the mAKAP anchoring protein under each experimental condition, suggesting that the reduction in phosphodiesterase activity is not a consequence of displacing the enzyme from the mAKAP complex (Fig. 1g, bottom panel). ERK activity was also measured in mAKAP-immunoprecipitated complexes (Fig. 1h, column 1), and an increase of 3.9 ± 0.7-fold (n = 3, P < 0.0007) over the IgG control (immunoprecipitation with IgG) was observed (data not shown). PD98059 (2 μM) blocked mAKAP-associated ERK activity (Fig. 1h, column 2, P < 0.0001). The PKA inhibitor PKI 5–24 peptide (50 nM) had no significant effect on ERK activity (Fig. 1h, column 3). Thus, mAKAP-associated ERK activity suppresses anchored PDE4D3 activity.

To determine which ERK family members might suppress mAKAP-associated PDE4D3, we performed western blot analysis on mAKAP immunoprecipitates from heart extracts. An 80-kDa protein that co-purified with mAKAP was detected with an antibody that recognizes all ERK family members and also with an ERK5-specific antibody (Fig. 1i, top and middle panels, lane 3). ERK5 was enriched in mAKAP immune complexes, but the 45-kDa ERK1/2 kinase was not (Fig. 1i, top panel, lane 1). The upstream kinase MEK5 (refs 14, 15) also co-precipitated with mAKAP (Fig. 1i, bottom panel). Immunofluorescence detection of mAKAP and ERK5 at the perinuclear membranes of hypertrophic RNVs confirmed the in situ assembly of this signalling complex[16] (Supplementary Fig. S1).

We wanted to determine whether anchored PKA and ERK5 facilitate bidirectional regulation of the mAKAP-associated phosphodiesterase, hence controlling localized cAMP metabolism. Glutathione S-transferase (GST) pulldowns from heart extracts established the formation of a mAKAP–PDE4D3–ERK5 ternary complex (Supplementary Fig. S2). Cellular binding studies showed that PDE4D3 acts as an adaptor protein linking ERK5 to the mAKAP complex. This was confirmed when a mutant PDE4D3 form unable to bind ERK kinases (the KIM/FQF double mutant, see Methods[17]) could not recruit ERK5 to mAKAP (Supplementary Figs S3–S5). Thus, ERK5 is well positioned to suppress PDE4D3 activity and influence localized accumulation of cAMP.

cAMP modulates ERK signalling in a context-specific manner[18]. cAMP activates ERK in neuronally derived cell lines, but it inhibits ERK in certain fibroblasts and kidney cells[19,20]. We evaluated crosstalk between mAKAP-anchored PKA and ERK5 in RNVs. When ERK was activated with 10% serum before immunoprecipitation of the mAKAP complex, mAKAP-associated ERK activity was increased 2.9 ± 0.6-fold ($n = 3$, $P < 0.0003$) over controls (Fig. 2a, column 2). However, pretreatment with forskolin ($20 \mu M$) to elevate intracellular cAMP resulted in an $89 \pm 8\%$ reduction in the serum-dependent activation of the mAKAP-associated ERK5 pool ($n = 3$, $P < 0.0004$; Fig. 2a, column 3). To our surprise, the PKA antagonist H89 ($10 \mu M$) did not overcome the cAMP-dependent suppression of ERK5 activity (Fig. 2a, column 4). Similar results were obtained using two other well-characterized PKA inhibitors, KT5720 ($1 \mu M$) and Rp-cAMPs ($1 mM$; Fig. 2a, columns 5, 6). Thus, the cAMP-dependent block of ERK5 activity was independent of PKA. Control experiments show that this effect was not a consequence of displacing ERK5 from the mAKAP complex (Fig. 2a, bottom). Therefore, another cAMP

effector within the mAKAP complex may function to suppress ERK5 activation.

One such candidate is Epac1 (exchange protein directly activated by cAMP), a cAMP-dependent guanine nucleotide exchange factor for the small G-protein Rap1 (refs 21, 22). Epac1 co-purified with mAKAP from heart extracts, but was not detected in an IgG control immunoprecipitation (Fig. 2b). Immunofluorescence techniques detected Epac1 at the perinuclear membranes of hypertrophic RNVs, where mAKAP is also found (Fig. 2c–e).

The cAMP analogue 8-CPT-2′-O-Me-cAMP was used to assess whether Epac1 is the cAMP effector that inhibits mAKAP-associated ERK5. This compound, also called 007, is a potent and selective activator of Epac proteins, with up to 300-fold selectivity over the R subunits of PKA[23]. Treatment of RNVs with 007 alone resulted in the inhibition of ERK5 activity in mAKAP immune complexes (Fig. 2f, column 3, $n = 3$, $P < 0.0004$). KT5720 did not increase the effect of 007 (Fig. 2f, column 4), emphasizing that PKA does not have an additive effect on cAMP-dependent suppression of ERK5. Further biochemical experiments demonstrated that PDE4D3 recruits Epac1 to the mAKAP complex (Supplementary Figs S6–S8). This permits firm control of cAMP concentrations in the vicinity of Epac1, thereby regulating its guanine nucleotide exchange activity.

Epac1 is an effector protein of Rap1, a member of the Ras family of small G-proteins[21,22]. Rap1 signalling is attenuated by the GTPase activating protein RapGAP[24]. Adenovirus-mediated expression of constitutively active RapGAP in heart cells blocked Rap1 and, consequently, cAMP-mediated suppression of ERK5 activity (Fig. 2g, columns 1–3, $n = 4$, $P < 0.007$). Treatment with the PKA inhibitor KT5720 did not reverse this effect (Fig. 2g, column 4).
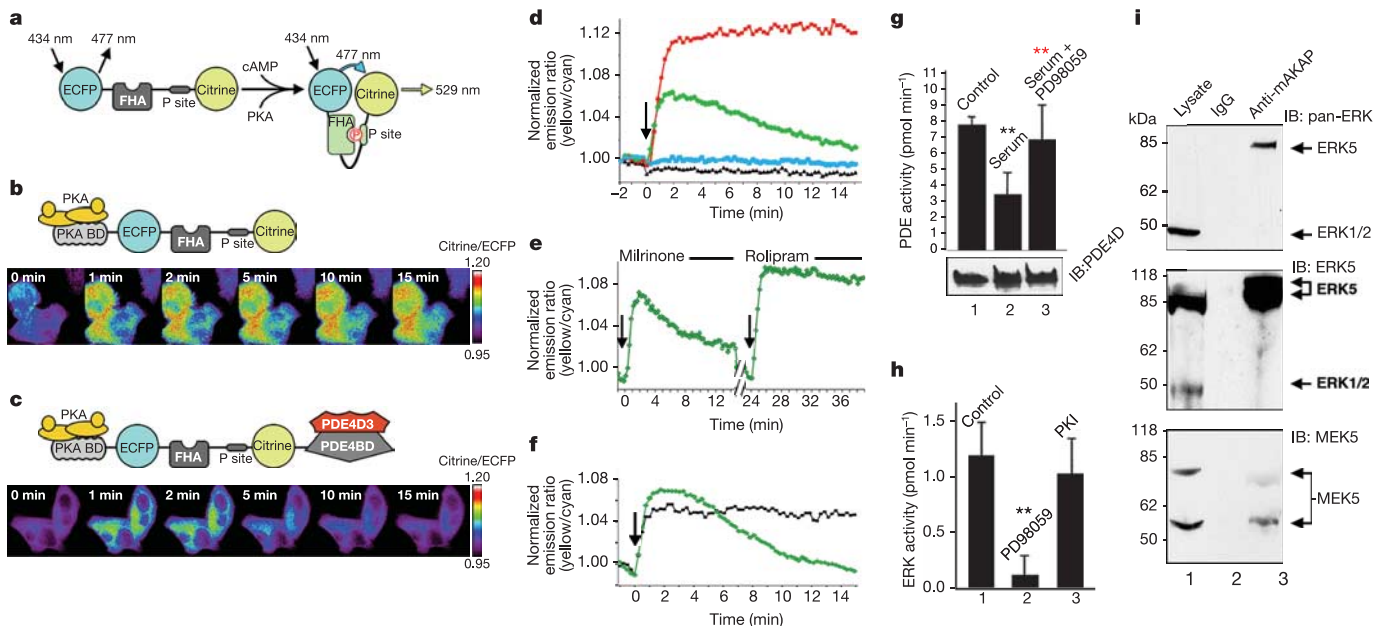

Figure 1 | Bidirectional control of the mAKAP-associated PDE4D3 activity. a, The modular composition and action of AKAR2. **b**, Schematic of AKAR2–PKA (top), and pseudo-coloured images of FRET changes in AKAR2–PKA-expressing HeLa cells stimulated with cAMP for 15 min (bottom). **c**, Schematic of AKAR2–PKA–PDE (top), and pseudo-coloured images of FRET changes in AKAR2–PKA–PDE-expressing HeLa cells stimulated with cAMP for 15 min (bottom). **d**, FRET measurements for AKAR–PKA (red, $n = 10$), AKAR–PKA–PDE (green, $n = 13$), AKAR–PKA + H89 (blue, $n = 10$) and AKAR–PKA–PDE + H89 (black, $n = 7$) for 15 min after cAMP stimulation with forskolin (arrow). **e**, FRET traces ($n = 10$) using the AKAR–PKA–PDE reporter after application of the PDE3 inhibitor milrinone (0–12 min) and the PDE4 inhibitor rolipram

(24–36 min). Stimulation with cAMP was at 0 and 24 min (arrows). **f**, FRET measurements from HeLa cells expressing the AKAR–PKA–PDE reporter in the presence (black, $n = 11$) or absence (green, $n = 7$) of a dominant active MEK5 for 15 min after cAMP stimulation with forskolin (arrow). **g**, Phosphodiesterase activity ($n = 4$) in mAKAP immune complexes isolated from RNVs. Treatment conditions are indicated. IB, immunoblot. **h**, ERK activity in mAKAP complexes immunoprecipitated from heart extracts ($n = 3$). Treatments with kinase inhibitors are indicated. Error bars in **g**, **h** show s.e.m. P values <0.01 are indicated by asterisks (black, relative to control; red, relative to sample). **i**, Co-precipitated ERK was detected by immunoblot of mAKAP complexes from heart extracts using pan-ERK (top), ERK5-specific (middle) and MEK5-specific (bottom) antibodies.

Other control experiments demonstrated that adenoviral expression of β-galactosidase did not affect cAMP-dependent suppression of anchored ERK5 activity (Fig. 2h, $n = 3$, $P < 0.009$). Collectively, the data in Fig. 2 suggest that cAMP-dependent activation of Epac1 mobilizes a Rap1 signalling pathway, leading to inhibition of ERK5 in the mAKAP complex.
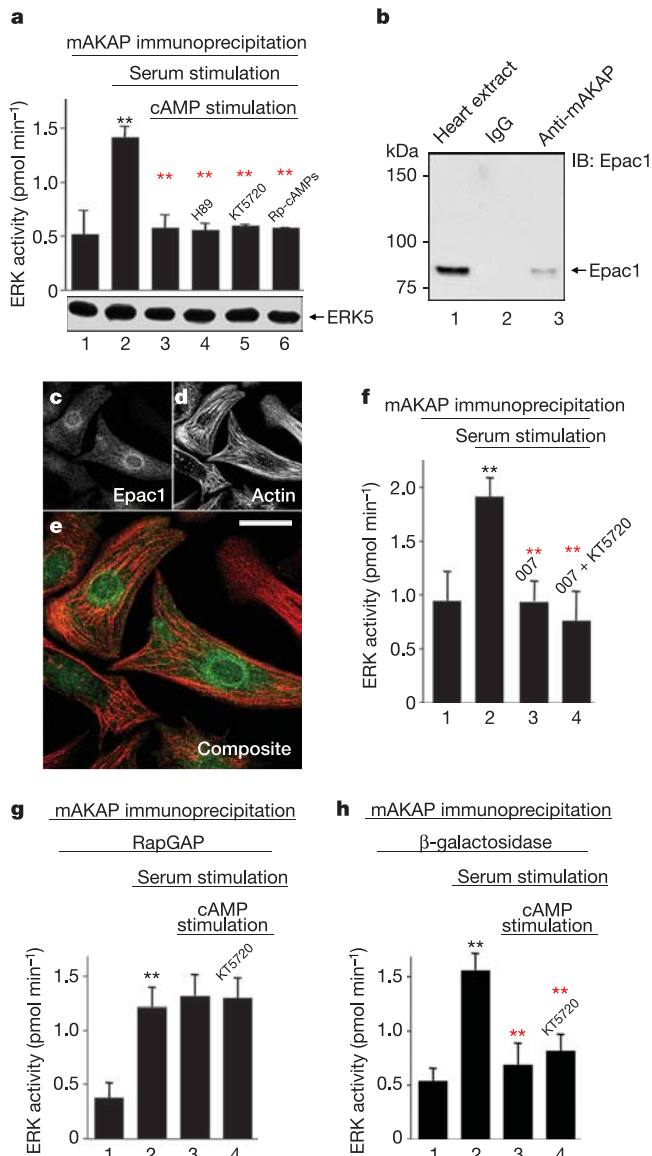
Cytokines, including leukaemia inhibitory factor (LIF), activate ERK5 in RNVs to induce eccentric cardiac hypertrophy, an increase in cell size and length[25]. LIF treatment for 24 h enhanced RNV cell size by 1.6-fold over controls (Fig. 3a–c, $n = 11$ independent experiments). This effect was blocked when ERK kinases were inhibited by PD98059 or if Epac1 was activated by 007, and was partially blocked on PDE4 inhibition with rolipram (Fig. 3c, columns 3–5). Plasmid-based RNA interference of mAKAP also suppressed LIF-mediated changes in RNV size compared with controls (Fig. 3d and Supplementary Fig. S9). The LIF response was rescued in RNVs
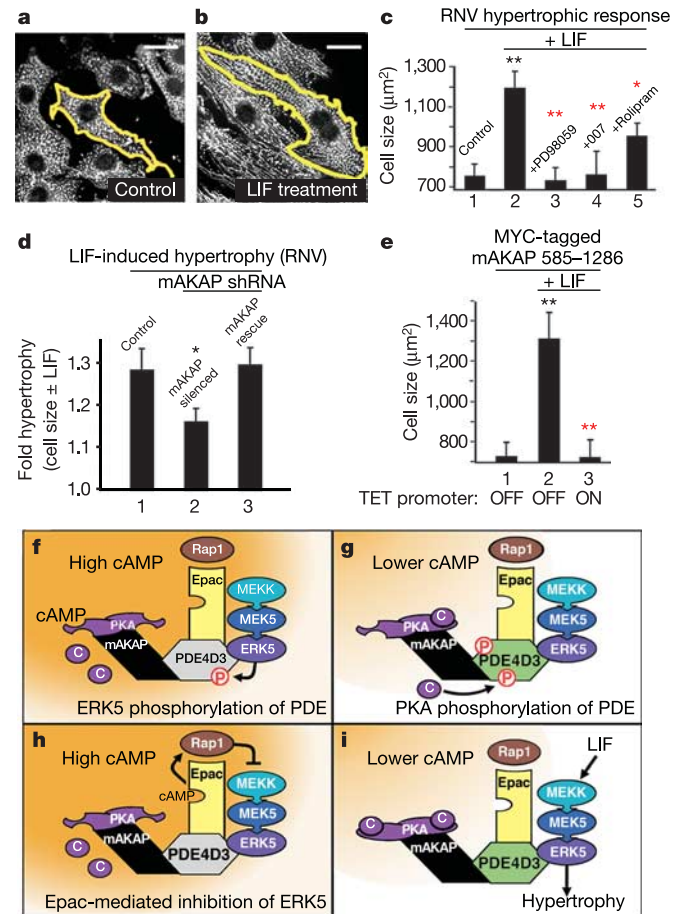

Figure 2 | Epac1 suppresses mAKAP-associated ERK5 activity. a, Serum-stimulated mAKAP-associated ERK5 activity ($n = 3$) in parallel cultures pretreated with forskolin to elevate cAMP (columns 2, 3) or in the presence of the PKA inhibitors H89, KT5720 or Rp-cAMPs (columns 4–6). Bottom panel shows the amount of ERK5 detected in each sample. **b**, Immunoblot detection of Epac1 in mAKAP immune complexes from rat heart extracts. **c–e**, Fluorescent staining of hypertrophic RNVs with an anti-Epac1 antibody (**c**) and Alexa 568 phalloidin to reveal the actin cytoskeleton (**d**). Composite image (**e**) shows the distribution of Epac1 (green) and actin (red). Scale bar, 20 μm. **f**, The mAKAP complex was immunoprecipitated from cultured RNVs following serum stimulation to activate ERK. Before serum stimulation, parallel cultures were pretreated with either the Epac-selective activator 007 or KT5720 ($n = 3$). **g, h**, Serum-stimulated mAKAP-associated ERK activity in cells expressing constitutively active RapGAP (**g**, $n = 4$) or control β-galactosidase (**h**, $n = 3$). Stimulation of intracellular cAMP or treatment with the kinase inhibitor KT5720 is indicated. P values <0.01 are indicated by asterisks (black, relative to control; red, relative to sample). Error bars in **f–h** show s.e.m.

Figure 3 | The mAKAP complex facilitates cytokine-induced cardiac hypertrophy. a–c, Leukaemia inhibitory factor (LIF) induces changes in RNV size. The outline of a rat neonatal ventriculocyte from control (**a**) and LIF-treated (**b**) samples is presented. Scale bar, 20 μm. **c**, Quantification of cell size in control RNVs (lane 1, $n = 11$) and LIF-treated RNVs (lane 2 ($n = 11$) and lanes 3–5). Pharmacological manipulation of ERK5 (PD98095, $n = 4$), Epac1 (007, $n = 4$) or PDE4 (rolipram, $n = 7$) activity is indicated. **d**, Expression of mAKAP was suppressed by RNA interference. Quantification of LIF-induced hypertrophy (cell size ± LIF) in control RNVs (lane 1, $n = 12$), mAKAP-silenced RNVs (lane 2, $n = 19$) and RNVs rescued with a variant of mAKAP resistant to the shRNA (lane 3, $n = 13$). **e**, Displacement of mAKAP from the nuclear membrane was achieved by overexpression of an mAKAP targeting domain fragment using the TET OFF inducible promoter. Quantification of cell size from control (lane 1, $n = 3$), from LIF-stimulated RNV controls (lane 2, $n = 4$), and from LIF-stimulated cells expressing the mAKAP 585–1286 fragment (lane 3, $n = 4$). P values are indicated by asterisks (black, relative to control; red, relative to sample): single asterisk, $P < 0.05$; two asterisks, $P < 0.01$. Error bars in **c–e** show s.e.m. **f–i**, Schematics highlighting the main findings of this study. **f**, ERK5 phosphorylation of PDE4D3 shuts down cAMP metabolism. **g**, PKA phosphorylation of PDE4D3 enhances cAMP metabolism. **h**, Activation of Epac mobilizes Rap1 to suppress ERK5 activation. **i**, Low cAMP represses the Epac-mediated block of ERK5, allowing cardiac hypertrophy.

expressing a variant of mAKAP resistant to the short hairpin (sh)RNA (Fig. 3d, column 3). Finally, displacement of mAKAP from the perinuclear membrane with an inducible competing mAKAP fragment (residues 585–1286) blocked LIF-induced RNV growth (Fig. 3e and Supplementary Fig. S10). Collectively, these data suggest that mAKAP organizes a cAMP-responsive network containing PDE4D3, Epac1 and ERK5 that modulates cardiomyocyte size. Similar results were observed when atrial natriuretic factor (ANF) expression was monitored as an independent index of hypertrophy (Supplementary Figs S11 and S12).

β-adrenergic agonists that elevate intracellular cAMP control the strength, duration and frequency of heart contraction. Cell imaging experiments in cardiomyocytes have revealed transient microdomains of cAMP where PKA becomes active[26,27]. Our FRET data show that co-localization of PKA and a phosphodiesterase generate localized pulses of cAMP. A variety of cAMP-responsive events that have different durations and are responsive to different thresholds of cAMP can emanate from the same microdomain. This is particularly relevant for mAKAP signalling complexes, which contain three functionally distinct cAMP-dependent enzymes (PKA, PDE4D3 and Epac1). PKA responds to nanomolar concentrations of cAMP, and would become active early in a second messenger response. PDE4D3 (K_m 1–4 μM) and Epac1 (K_d 4 μM) would only become activated once cAMP concentrations reached micromolar levels[4]. Conversely, inactivation of PDE4D3 and Epac1 would precede PKA holoenzyme reformation as cAMP levels decline. Furthermore, Epac1 suppresses mAKAP-associated ERK5 activity in a PKA-independent manner. This is consistent with the idea that Epac proteins provide the cAMP-dependent link to ERK signalling events through Rap1[22,23,28].

In conclusion, mAKAP and PDE4D3 create an integrated and internally regulated signalling network. mAKAP anchors PKA and directs the cellular localization of the complex, while PDE4D3 serves as the adaptor protein for Epac1 and ERK5. The key regulatory enzyme is PDE4D3. ERK phosphorylation of PDE4D3 decreases the phosphodiesterase activity, thereby favouring local accumulation of cAMP and subsequent PKA activation (Fig. 3f) and Epac1 activation (Fig. 3h). Conversely, PKA phosphorylation of PDE4D3 increases its affinity for mAKAP[9] and its V_{max} for cAMP[10], decreasing the local cAMP concentration (Fig. 3g). This ultimately sustains ERK5 activity by repressing Epac1-mediated inhibition of ERK5 (Fig. 3i). This configuration creates a complex in which transduction enzymes from distinct pathways are spatially organized to exploit the temporal constraints of cAMP action.

METHODS

Antibodies. Primary antibodies used were monoclonal anti-pan-ERK (Transduction Labs), monoclonal anti-MEK5 (Transduction Labs), monoclonal anti-pan-PDE4D (ICOS), rabbit anti-ERK5 (StressGen), monoclonal anti-9E10-Myc (Upstate), rabbit anti-mAKAP (VO54), rabbit anti-Epac1 (Santa Cruz), mouse anti-α-actinin (Sigma) and rabbit anti-rat ANF (USB). Donkey HRP-conjugated (Jackson ImmunoResearch) and Alexa-conjugated (Molecular Probes) secondary antibodies were used.

AKAR–PKA and AKAR–PKA–PDE. Plasmids (pcDNA4) encoding AKAR–PKA or AKAR–PKA–PDE were derived from the original AKAR2 construct provided by R. Tsien. A DNA fragment encoding the consensus RII binding peptide from AKAP*is* (A-kinase anchoring protein-*in silico*: a 22-amino-acid peptide that is a high-affinity PKA-anchoring anagonist developed using a bioinformatic approach) following a Kozak sequence was generated by polymerase chain reaction (PCR). This fragment was ligated at the 5′ end of AKAR2 to generate AKAR–PKA. The AKAR–PKA–PDE reporter was constructed by ligating a fragment encoding residues 1286–1831 of mAKAP to the 3′ end of the AKAR–PKA coding region.

Cell culture. Preparation of primary RNVs and treatment to induce hypertrophy was as previously described[16].

Live cell imaging. HeLa cells grown on glass coverslips were transfected with vectors encoding AKAR–PKA or AKAR–PKA–PDE using Lipofectamine 2000. After incubation at 37 °C for 18–48 h, cells were washed twice with Hank's balanced salt solution, mounted in a Ludin chamber (Life Imaging Services) and

imaged using a Leica AS MDW workstation. Images were acquired using a Leica DM IRE2 microscope equipped with a CoolSNAP-HQ charge-coupled device camera (Roper Photometrics). This device was equipped with a Dual-view module (Optical Insights), D465/30 and HQ535/30 emission filters (Chroma) and a 505dcxr dichroic mirror (Chroma). CFP and YFP images were acquired simultaneously, aligned, background-corrected and analysed using FRET Applicator software (Leica). Exposure time was from 250–1,000 ms, and images were taken every 15 s. Treatment with the PKA inhibitor H89 or isoform-specific PDE inhibitors preceded cAMP stimulation with forskolin by 10 min.

Expression constructs. Plasmids encoding wild-type PDE4D3 and mutant PDE4D3 (K455A/K456A/F597A/Q598A/F599A; this is the KIM/FQF double mutant) forms were from M. Houslay. pcDNA3 expression vectors encoding MYC-tagged ERK5 and Epac1, and a RAP-GAP adenovirus, were provided by P. Stork. For GST–PDE4D3 and GST–ERK5, complementary DNAs were subcloned into PGEX-4T2. shRNA vectors incorporated double-stranded hairpin oligonucleotides based on rat mAKAP messenger RNA sequence (NCBI GI:5070430, base pairs 7210–7228) under the direction of the U6 promoter: mAKAP shRNA (sense strand), 5′-GACGAACCTTCCTTCCGAATTCAAGA GATTCGGAAGGAAGGTTCGTCTTTTT-3′; control shRNA (sense strand) 5′-GACGAACC**CCTG**TTCCGAATTCAAGAGATTCGGAA**CAGG**GGTTCG TCTTTTT-3′. Bold base pairs in the control shRNA are different from the wild-type mAKAP shRNA. Rescue experiments were performed with a full-length MYC–His rat mAKAP lacking the shRNA recognition sequence that resides in the 3′ untranslated region of the mAKAP message.

Enzyme assays. PDE activity was measured by the method in ref. 29, and PKA activity was measured as previously described[8]. ERK assays were performed on immunoprecipitates from heart extracts and RNVs. Immunoprecipitates were washed three times in HSE buffer before the addition of inhibitors, 25 μl H₂O and 25 μl ERK assay buffer (80 mM HEPES pH 7.4, 80 mM MgCl₂, 0.2 μM ATP, 2 mM sodium orthovanadate, 20 mM NaF, 1 μg tyrosine hydroxylase peptide (BioSource) and 10 μCi γ-³²ATP). After 30 min incubation at 30 °C, the reaction mixture was spotted onto phosphocellulose strips and extensively washed in 75 mM phosphoric acid. Filters were washed in 95% ethanol, air-dried and counted by liquid scintillation.

RNVs were serum-starved for 16 h before the addition of either 20 μM PD98059, the PKA inhibitors H 89 (10 μM), KT5720 (1 μM) or Rp-cAMPs (1 mM), for 1 h. Forskolin (20 μM) and 3-isobutyl-1-methylxanthine (IBMX, 75 μM) were then added for 20 min. For 8-CPT-2′-O-Me-cAMP treatment (50 μM, the Epac-selective cAMP analogue 007), cells were not exposed to forskolin. Cells were stimulated with 10% fetal calf serum for 10 min, lysed in 1 ml HSE buffer containing 50 mM NaF, 1 mM sodium orthovanadate, 0.1 μM okadaic acid and 0.1 μM cyclosporine, and immunoprecipitations were performed as described above.

H9C2 heart cells were incubated with adenoviral constructs of Rap1GAP1 or β-galactosidase at a multiplicity of infection (MOI) of 50 for 48 h. The cells were treated as described above before the addition of forskolin/IBMX and before serum stimulation.

Immunocytochemistry and microscopy. Fixation and staining of RNVs were as previously described[8]. To determine the effect of shRNA expression on cellular hypertrophy, myocytes were co-transfected with pTRE-U6 mAKAP shRNA or control shRNA plasmid, pEGFPN3 green fluorescent protein expression plasmid (Clontech) and either pBluescript carrier DNA or pcDNA3.1 MYC–His mAKAP expression vector for rescue experiments. Cells were stained with primary and Alexa-conjugated specific secondary antibodies. Anti-α-actinin stained sarcomeric Z-disks to distinguish myocytes from contaminating fibroblasts. Images were acquired using a Leica DMRA fluorescent microscope. Cell size was measured using the method in ref. 30. Data are presented as the average mean cell area ± s.e.m. *P*-values were determined using a two-tailed Student's *t*-test.

1. Walsh, D. A., Perkins, J. P. & Krebs, E. G. An adenosine 3′,5′-monophosphate-dependent protein kinase from rabbit skeletal muscle. *J. Biol. Chem.* **243**, 3763–3765 (1968).

2. Su, Y. *et al.* Regulatory subunit of protein kinase A: structure of deletion mutant with cAMP binding proteins. *Science* **269**, 807–813 (1995).

3. Bos, J. L. Epac: a new cAMP target and new avenues in cAMP research. *Nature Rev. Mol. Cell Biol.* **4**, 733–738 (2003).

4. Beavo, J. A. & Brunton, L. L. Cyclic nucleotide research—still expanding after half a century. *Nature Rev. Mol. Cell Biol.* **3**, 710–718 (2002).

5. Houslay, M. D. & Adams, D. R. PDE4 cAMP phosphodiesterases: modular enzymes that orchestrate signalling cross-talk, desensitization and compartmentalization. *Biochem. J.* **370**, 1–18 (2003).

6. Perry, S. J. *et al.* Targeting of cyclic AMP degradation to β2-adrenergic receptors by β-arrestins. *Science* **298**, 834–836 (2002).

7. Verde, I. *et al.* Myomegalin is a novel protein of the Golgi/centrosome that interacts with a cyclic nucleotide phosphodiesterase. *J. Biol. Chem.* **276**, 11189–11198 (2001).

8. Dodge, K. L. *et al.* mAKAP assembles a protein kinase A/PDE4 phosphodiesterase cAMP signalling module. *EMBO J.* **20**, 1921–1930 (2001).

9. Carlisle Michel, J. J. *et al.* PKA phosphorylation of PDE4D3 facilitates recruitment of the mAKAP signalling complex. *Biochem. J.* **381**, 587–592 (2004).

10. Sette, C. & Conti, M. Phosphorylation and activation of a cAMP-specific phosphodiesterase by the cAMP-dependent protein kinase. *J. Biol. Chem.* **271**, 16526–16534 (1996).

11. Wong, W. & Scott, J. D. AKAP signalling complexes: Focal points in space and time. *Nature Rev. Mol. Cell Biol.* **5**, 959–971 (2004).

12. Zhang, J., Ma, Y., Taylor, S. S. & Tsien, R. Y. Genetically encoded reporters of protein kinase A activity reveal impact of substrate tethering. *Proc. Natl Acad. Sci. USA* **98**, 14997–15002 (2001).

13. Hoffmann, R., Baillie, G. S., MacKenzie, S. J., Yarwood, S. J. & Houslay, M. D. The MAP kinase ERK2 inhibits the cyclic AMP-specific phosphodiesterase HSPDE4D3 by phosphorylating it at Ser579. *EMBO J.* **18**, 893–903 (1999).

14. Zhou, G., Bao, Z. Q. & Dixon, J. E. Components of a new human protein kinase signal transduction pathway. *J. Biol. Chem.* **270**, 12665–12669 (1995).

15. English, J. M., Vanderbilt, C. A., Xu, S., Marcus, S. & Cobb, M. H. Isolation of MEK5 and differential expression of alternatively spliced forms. *J. Biol. Chem.* **270**, 28897–28902 (1995).

16. Kapiloff, M. S., Schillace, R. V., Westphal, A. M. & Scott, J. D. mAKAP: an A-kinase anchoring protein targeted to the nuclear membrane of differentiated myocytes. *J. Cell Sci.* **112**, 2725–2736 (1999).

17. MacKenzie, S. J., Baillie, G. S., McPhee, I., Bolger, G. B. & Houslay, M. D. ERK2 mitogen-activated protein kinase binding, phosphorylation, and regulation of the PDE4D cAMP-specific phosphodiesterases. The involvement of COOH-terminal docking sites and NH$_2$-terminal UCR regions. *J. Biol. Chem.* **275**, 16609–16617 (2000).

18. Pearson, G. W. & Cobb, M. H. Cell condition-dependent regulation of ERK5 by cAMP. *J. Biol. Chem.* **277**, 48094–48098 (2002).

19. Cook, S. J. & McCormick, F. Inhibition by cAMP of Ras-dependent activation of Raf. *Science* **262**, 1069–1072 (1993).

20. Vaillancourt, R. R., Gardner, A. M. & Johnson, G. L. B-Raf-dependent regulation of the MEK-1/mitogen-activated protein kinase pathway in PC12 cells and regulation by cyclic AMP. *Mol. Cell. Biol.* **14**, 6522–6530 (1994).

21. de Rooij, J. *et al.* Epac is a Rap1 guanine-nucleotide-exchange factor directly activated by cyclic AMP. *Nature* **396**, 474–477 (1998).

22. Kawasaki, H. *et al.* A family of cAMP-binding proteins that directly activate Rap1. *Science* **282**, 2275–2279 (1998).

23. Enserink, J. M. *et al.* A novel Epac-specific cAMP analogue demonstrates independent regulation of Rap1 and ERK. *Nature Cell Biol.* **4**, 901–906 (2002).

24. Rubinfeld, B. *et al.* Molecular cloning of a GTPase activating protein specific for the Krev-1 protein p21rap1. *Cell* **65**, 1033–1042 (1991).

25. Nicol, R. L. *et al.* Activated MEK5 induces serial assembly of sarcomeres and eccentric cardiac hypertrophy. *EMBO J.* **20**, 2757–2767 (2001).

26. Zaccolo, M. & Pozzan, T. Discrete microdomains with high concentration of cAMP in stimulated rat neonatal cardiac myocytes. *Science* **295**, 1711–1715 (2002).

27. Mongillo, M. *et al.* Fluorescence resonance energy transfer-based analysis of cAMP dynamics in live neonatal rat cardiac myocytes reveals distinct functions of compartmentalized phosphodiesterases. *Circ. Res.* **95**, 67–75 (2004).

28. Laroche-Joubert, N., Marsy, S., Michelet, S., Imbert-Teboul, M. & Doucet, A. Protein kinase A-independent activation of ERK and H,K-ATPase by cAMP in native kidney cells: role of Epac I. *J. Biol. Chem.* **277**, 18598–18604 (2002).

29. Beavo, J. A., Bechtel, P. J. & Krebs, E. G. Preparation of homogeneous cyclic AMP-dependent protein kinase(s) and its subunits from rabbit skeletal muscle. *Methods Enzymol.* **38**, 299–308 (1974).

30. Kodama, H. *et al.* Significance of ERK cascade compared with JAK/STAT and PI3-K pathway in gp130-mediated cardiac hypertrophy. *Am. J. Physiol. Heart Circ. Physiol.* **279**, H1635–H1644 (2000).

31. Zhang, J., Hupfeld, C. J., Taylor, S. S., Olefsky, J. M. & Tsien, R. Y. Insulin disrupts β-adrenergic signalling to protein kinase A in adipocytes. *Nature* doi:10.1038/nature04140 (this issue).